crystals

MDPI

Article

Schiff Base Derivatives in Zinc(II) and Cadmium(II) Complexation with the *closo*-Dodecaborate Anion

Svetlana E. Nikiforova [1,*], Nadezhda A. Khan [1], Alexey S. Kubasov [1], Yurii V. Koshchienko [2], Anatolii S. Burlov [2], Lyudmila N. Divaeva [2], Lyudmila V. Goeva [1], Varvara V. Avdeeva [1], Elena A. Malinina [1] and Nikolay T. Kuznetsov [1]

[1] Kurnakov Institute of General and Inorganic Chemistry, Russian Academy of Sciences, Leninskii pr. 31, Moscow 119991, Russia; nadya.khan@mail.ru (N.A.K.)
[2] Institute of Physical and Organic Chemistry, Southern Federal University, pr. Stachki 194/2, Rostov-on-Don 344090, Russia; yvkoshienko@sfedu.ru (Y.V.K.); anatoly.burlov@yandex.ru (A.S.B.)
* Correspondence: korolencko0110@yandex.ru

Abstract: A series of Schiff base derivatives, namely *N*-(4-methoxyphenyl)-1-(1-methylbenzimidazol-2-yl)methanimine (L^1), 4-methoxy-*N*-[(1-methylbenzimidazol-2-yl)methyl]aniline (L^2), and 2-[(*E*)-(1-propylbenzimidazol-2-yl)iminomethyl]phenol (L^3), were synthesized. These compounds feature different linker groups, including –CH=N–, –CH_2–NH–, and –N=CH–, respectively. During the process of zinc(II) and cadmium(II) complexation in the presence of the *closo*-dodecaborate $[B_{12}H_{12}]^{2-}$ anion, it was observed that ligand L^3 underwent degradation. Consequently, two compounds were isolated, $[Zn(Bz\text{-}NH_2)_2(CH_3COO)_2]$ and $(HBz\text{-}NH_2)_2[B_{12}H_{12}]\cdot 2CH_3CN$, both containing 1-propyl-2-aminobenzimidazole (Bz-NH_2), which is a degraded fragment of the ligand. Several new zinc(II) and cadmium(II) coordination compounds were synthesized and characterized using various physicochemical analysis methods, including elemental analysis, IR, and UV spectroscopy. Additionally, X-ray diffraction and Hirshfeld surface analysis were performed for compounds $[Cd(L^2)_2(CH_3CN)(H_2O)][B_{12}H_{12}]$, $[Zn(Bz\text{-}NH_2)_2(CH_3COO)_2]$, and $(HBz\text{-}NH_2)_2[B_{12}H_{12}]\cdot 2CH_3CN$, as well as for ligand L^2.

Keywords: X-ray diffraction; benzimidazole derivatives; zinc(II); cadmium(II); Hirshfeld surface analysis

check for updates

Citation: Nikiforova, S.E.; Khan, N.A.; Kubasov, A.S.; Koshchienko, Y.V.; Burlov, A.S.; Divaeva, L.N.; Goeva, L.V.; Avdeeva, V.V.; Malinina, E.A.; Kuznetsov, N.T. Schiff Base Derivatives in Zinc(II) and Cadmium(II) Complexation with the *closo*-Dodecaborate Anion. *Crystals* **2023**, *13*, 1449. https://doi.org/10.3390/cryst13101449

Academic Editors: Saied M. Soliman, Assem Barakat and Ayman El-Faham

Received: 11 September 2023
Revised: 26 September 2023
Accepted: 27 September 2023
Published: 29 September 2023

1. Introduction

The remarkable properties of compounds that incorporate both benzimidazole derivatives [1–10] and *closo*-dodecaborate anions [11–19] have sparked significant interest among chemists. This interest arises from not only their potential practical applications, but also from a fundamental perspective. A judicious selection of synthetic conditions, including initial reagents, solvents, and other factors, plays a crucial role in obtaining stable compounds with the desired composition.

As of today, zinc(II) and cadmium(II) coordination compounds incorporating the *closo*-dodecaborate anion are relatively scarce, primarily consisting of various cationic complexes stabilized by the *closo*-borate anion or its derivatives. Among these complexes, compounds with coordinated solvent molecules $[M(H_2O)_6][B_{12}X_{12}]$ (X is H and M is Zn(II) [20] or Cd(II) [21]; X is F and M is Zn(II) [22]), $[M(DMF)_6][B_{12}H_{12}]$ [23], $[Zn(CH_3CN)_6][B_{12}I_{12}]$ [24], as well as various salts $[ZnL_2][B_{12}I_{12}]$ (L is tris(2-methyl-6-pyridylmethyl)phosphine) [24], $[ZnL_6][B_{12}H_{12}]$ (L is 1-vinylimidazole) and $[ZnL_4][B_{12}H_{12}]$ (L is 1-allylimidazole) [25], [EtZn][An] and $Zn[An]_2$ (An is $[Me_3NB_{12}Cl_{11}]^-$, $[Pr_3NB_{12}H_5Cl_6]^-$, $[Bu_3NB_{12}H_4Cl_7]^-$, and $[Hex_3NB_{12}H_5Cl_6]^-$) [26], $[ZnL_2(\eta^2\text{-}O_2NO)]_2[L_2Zn(\mu\text{-}NO_3)_2ZnL_2][B_{12}H_{12}]_2$ (L is phen) and $[Cd(bpa)_2(CH_3CN)_2][B_{12}H_{12}]$ [23], $[ML_3][B_{12}H_{12}]$ (M is Zn(II), Cd(II) and L is bipy, phen [23]; M is Zn(II) and L is 1-methylbenzimidazo-2-yl-methyleneaniline or 1-ethyl-2-(4-methoxyphenyl)-azobenzimidazole) [27]) have been isolated.

Only three cadmium(II) complexes are currently known to feature the $[B_{12}H_{12}]^{2-}$ anion coordinated by a metal. These include unstable binuclear complex $[Cd(bpa)_2[\mu\text{-}B_{12}H_{12}]]_2$ [23] and mixed-ligand complexes with benzimidazole derivatives $[CdL_2[B_{12}H_{12}]]$ (L is 1-methylbenzimidazo-2-yl-methyleneaniline) and $[Cd(L^2)_2(CH_3CN)[B_{12}H_{12}]]$ (L is 1-ethyl-2-(4-methoxyphenyl)-azobenzimidazole) [27]. This fact allows us to assume that the formation of complexes with the coordinated *closo*-dodecaborate anion being a "soft" inorganic base is possible even for metals of "intermediate" acidity, according to Pearson′s concept. The crucial thing is to choose the right reagents and synthesis conditions.

In our current study, we have investigated the complexation of zinc(II) and cadmium(II) with the $[B_{12}H_{12}]^{2-}$ anion in the presence of Schiff base derivatives—specifically *N*-(4-methoxyphenyl)-1-(1-methylbenzimidazol-2-yl)methanimine (L^1), 4-methoxy-*N*-[(1-methylbenzimidazol-2-yl)methyl]aniline (L^2), and 2-[(*E*)-(1-propylbenzimidazol-2-yl) iminomethyl]phenol (L^3).

2. Materials and Methods

2.1. Materials

Acetonitrile (HPLC grade) was procured from Merck KGaA, Darmstadt, Germany and utilized without the need for additional purification. Complexes $[M(DMF)_6][B_{12}H_{12}]$ (M = Zn(II), Cd(II)) were synthesized according to the procedure outlined [23].

2.2. Synthesis of Organic Ligands L^1–L^3

2.2.1. *N*-(4-Methoxyphenyl)-1-(1-methylbenzimidazol-2-yl)methanimine (L^1)

A solution containing *para*-anisidine (0.62 g, 5 mmol) and 1-methyl-2-formylbenzimidazole (0.8 g, 5 mmol) in benzene (15 mL) (Warning! Highly toxic and carcinogenic) was heated to boiling for 2 h while concurrently distilling off water using a Dean-Stark apparatus. Upon cooling the solution, pale yellow crystals were formed, filtered, dried in air, and subsequently recrystallized from heptane. Melting point (mp) is 139–140 °C. Yield, 0.60 g (45%). **IR** (NaCl, cm^{-1}): ν(C=N) 1627, 1612, 1592, 1575; **^{1}H NMR** (600 MHz, $CDCl_3$, ppm): 3.82 (3H, s, OCH_3), 4.27 (3H, s, NCH_3), 6.94 (2H, d, *J* = 9.0 Hz, H3′, H5′), 7.30 (1H, d, *J* = 7.1 Hz, H4 or H7), 7.32 (2H, d, *J* = 9.0 Hz, H2′, H6′), 7.36 (1H, t, *J* = 7.5 Hz, H5), 7.41 (1H, d, *J* = 8.1 Hz, H7 or H4), 7.82 (1H, d *J* = 8.4 Hz, H6), 8.75 (1H, s, CH=N); **^{13}C NMR** (150 MHz, $CDCl_3$, ppm): 32.08, 55.49, 109.84, 114.59, 120.70, 122.51, 124.57, 137.25, 143.04, 148.06, 149.93, 159.33; elemental analysis calculated (%) for $C_{16}H_{15}N_3O$ (265.31): C 72.43, H 5.70, N 15.84; found: C 72.51, H 5.68, N 15.73.

2.2.2. 4-Methoxy-*N*-[(1-methylbenzimidazol-2-yl)methyl]aniline (L^2)

Sodium borohydride (0.28 g, 7.5 mmol) was introduced into a solution of L^1 in methanol (20 mL), and the mixture was stirred at room temperature for 2 h. Subsequently, water (10 mL) was added and methanol was evaporated. The resulting white precipitate was separated by filtration, washed with water, dried, and subjected to recrystallization from ethyl acetate. Melting point (mp) is 113–114 °C. Yield, 1.22 g (91%). **IR** (NaCl, Nujol mull, cm^{-1}): ν(NH) 3260; ν(C=N) 1612, 1605, 1586; **^{1}H NMR** (600 MHz, $CDCl_3$, ppm): 3.72 (3H, s, OCH_3), 3.73 (3H, s, NCH_3), 4.32 (1H, s, NH), 4.45 (2H, d, *J* = 4.1 Hz, CH_2), 6.72 (2H, d, *J* = 8.9 Hz, H2′, H6′), 6.79 (2H, d, *J* = 8.9 Hz, H3′, H5′), 7.23–7.30 (3H, m, H5, H6, H4 or H7), 7.74 (1H, d, *J* = 8.9 Hz, H7 or H4); **^{13}C NMR** (150 MHz, $CDCl_3$, ppm): 29.20, 42.13, 55.24, 108.55, 114.18, 118.98, 121.53, 122.10, 135.62, 141.23, 141.76, 151.36, 152.30; elemental analysis calculated (%) for $C_{16}H_{17}N_3O$ (267.33): C 71.89, H 6.41, N 15.72; found: C 71.91, H 6.48, N 15.68.

2.2.3. 2-[(*E*)-(1-Propylbenzimidazol-2-yl)iminomethyl]phenol (L^3)

A solution containing 1-propyl-2-aminobenzimidazole (1.75 g, 10 mmol) and salicylaldehyde (1.22 g, 10 mmol) in benzene (20 mL) was subjected to boiling for 1 h while simultaneously distilling off water using a Dean-Stark apparatus. Following this, benzene was removed via rotary evaporation. The resulting oily product was subsequently

recrystallized from hexane, yielding yellow crystals, which were then filtered, air-dried, and collected. Melting point (mp) is 75–76 °C. Yield, 2.2 g (79%). **IR** (NaCl, Nujol mull, cm^{-1}): ν(OH) ~3380–3250; ν(C=N) 1670, 1620, 1605, 1571, 1533. **^{1}H NMR** (600 MHz, $CDCl_3$, ppm): 0.96 (3H, t, *J* = 7.4 Hz, CH_3), 1.87–1.93 (2H, m, $CH_2\underline{CH_2}CH_3$), 4.24 (2H, t, *J* = 7.1 Hz, $\underline{CH_2}CH_2CH_3$), 6.98 (1H, t, *J* = 7.5 Hz, H3′), 7.03 (1H, d, *J* = 8.3 Hz, H6′), 7.25–7.29 (2H, m, H4′, H5′), 7.35 (1H, d, *J* = 9.0 Hz, H4), 7.44 (1H, t, *J* = 8.6 Hz, H5), 7.52 (1H, d, *J* = 9.1 Hz, H6), 7.72 (1H, d, *J* = 8.8 Hz, H7), 9.60 (1H, s, CH=N), 12.55 (1H, s, OH); **^{13}C NMR** (150 MHz, $CDCl_3$, ppm):10,92, 22.67, 43.87, 108.91, 116.78, 118.42, 119.34, 122.18, 133.45, 134.34, 141.11, 152.26, 161.21, 166.57; elemental analysis calculated (%) for $C_{17}H_{17}N_3O$ (279.34): C 73.10, H 6.13, N 15.04; found: C 73.15, H 6.10, N 15.10.

2.3. Synthesis of Zinc(II) and Cadmium(II) Complexes

A solution of organic ligand L (L^1, L^2, or L^3) (6 mmol) in CH_3CN (10 mL) was added to a solution of $[M(DMF)_6][B_{12}H_{12}]$ (M = Zn(II), Cd(II)) (3 mmol) in the same volume of the same solvent. The precipitate formed after standing the reaction mixture in air was filtered, air-dried, and collected.

2.3.1. $[Cd(L^1)_2[B_{12}H_{12}]]$ (Compound **1**)

Yellow precipitate of **1** was obtained by allowing the reaction solution containing $[Cd(DMF)_6][B_{12}H_{12}]/L^1$ to evaporate for 48 h. Yield, 69%. **IR** (NaCl, Nujol mull, cm^{-1}): ν(BH) 2506, 2477; $\nu(BH)_{MHB}$ 2407; ν(C=N) 1650, 1623, 1609, 1579; elemental analysis calculated (%) for $CdC_{32}H_{42}N_6O_2B_{12}$ (784.86): Cd 14.32, C 48.97, H 5.39, N 10.71, B 16.5; found: Cd 14.39, C 48.91, H 5.47, N 10.62, B 16.1.

2.3.2. $[Cd(L^2)_2(CH_3CN)(H_2O)][B_{12}H_{12}]$ (Compound **2**)

Colorless single crystals of **2** suitable for X-ray diffraction studies were obtained by allowing the reaction solution containing $[Cd(DMF)_6][B_{12}H_{12}]/L^2$ to evaporate for 48 h. Yield, 65%. **IR** (NaCl, Nujol mull, cm^{-1}): $\nu(OH)_{H2O}$ 3583, ~3513; ν(NH) 3257; ν(BH) 2479, 2461, 2436; ν(C=N) 1651, 1618, 1597; elemental analysis calculated (%) for $CdC_{34}H_{51}N_7O_3B_{12}$ (847.95): Cd 13.26, C 48.16, H 6.06, N 11.56, B 15.3; found: Cd 13.32, C 48.09, H 6.14, N 11.61, B 14.8.

2.3.3. $[Zn(Bz\text{-}NH_2)_2(CH_3COO)_2]$ (Compound **3**)

Light yellow single crystals of **3** suitable for X-ray diffraction studies were obtained by allowing the reaction solution containing $[Zn(DMF)_6][B_{12}H_{12}]/L^3$ to evaporate for 48 h. Yield, 62%. **IR** (NaCl, Nujol mull, cm^{-1}): $\nu_{as}(NH)_{NH2}$ 3333, $\nu_s(NH)_{NH2}$ 3189; $\nu(CO)_{COO}$ 1663; ν(C=N) + $\delta(NH_2)$ 1617, 1562; elemental analysis calculated (%) for $ZnC_{24}H_{32}N_6O_4$ (533.94): Zn 12.25, C 53.99, H 6.04, N 15.74; found: Zn 12.31, C 53.92, H 5.98, N 15.79.

2.3.4. $(HBz\text{-}NH_2)_2[B_{12}H_{12}]\cdot 2CH_3CN$ (Compound **4**·$2CH_3CN$) + Cadmium(II) Complex with Salicylaldehyde

An inhomogeneous white precipitate containing colorless single crystals of salt **4**·$2CH_3CN$ suitable for X-ray diffraction studies was obtained by allowing the reaction solution containing $[Cd(DMF)_6][B_{12}H_{12}]/L^3$ to evaporate for 48 h. Yield, ~55%. **IR** (NaCl, Nujol mull, cm^{-1}): ν(OH) 3605, 3566; $\nu(NH)_{NH+NH2}$ 3340, 3334, 3298, 3225; ν(BH) 2470; ν(C=O) 1663; ν(C=N) + $\delta(NH_2)$ 1640, 1542.

2.4. Elemental Analysis

Carbon, hydrogen, and nitrogen content was analyzed using a Carlo ErbaCHNS-3 FA 1108 automated elemental analyzer (Carlo Erba Instruments, Milan, Italy). Zinc(II), cadmium(II), and boron content was determined on an iCAP 6300 Duo ICP emission spectrometer with inductively coupled plasma (Thermo Scientific, Waltham, MA, USA).

2.5. IR Spectroscopy

IR spectra of compounds were recorded on a Lumex Infralum FT-02 Fourier-transform spectrophotometer (Lumex, St. Petersburg, Russia). The measurements were recorded in the range of 4000–600 cm^{-1} at a resolution of 1 cm^{-1}. Samples were prepared as Nujol mulls; for measurements, NaCl pellets were used. IR spectra of compounds are shown in Supplementary Materials (Figures S1–S4).

2.6. UV Spectroscopy

UV-vis absorption spectra of ligands L^1–L^3 and compounds **1**–**3** as glycerol suspensions were recorded using a SF 103 spectrophotometer (Akvilon, Moscow, Russia) in the region of 200–700 nm. UV-vis absorption spectra are shown in Supplementary Materials (Figures S5–S7).

2.7. ^{1}H and ^{13}C NMR Spectroscopy

^{1}H and ^{13}C NMR spectra of organic ligands L^1–L^3 were measured on a Bruker AVANCE-600 spectrometer (Bruker AXC, Inc., Karlsruhe, Germany) in $CDCl_3$ at 600 and 150 MHz, respectively, with internal deuterium stabilization. The chemical shifts of the ^{1}H nuclei are given relative to the residual signals of the deuterosolvent. Tetramethylsilane was used as an external standard. ^{1}H and ^{13}C NMR spectra are present in Supplementary Materials (Figures S8–S13).

2.8. X-ray Diffraction

The single-crystal X-ray diffraction data for compounds **2**–**4**·2CH_3CN and ligand L^2 were collected using a three-circle Bruker D8 Venture diffractometer (Bruker AXS Inc., Karlsruhe, Germany). The studies were performed at the Kurnakov Institute of General and Inorganic Chemistry, Russian Academy of Sciences. The data were collected using the φ and ω scan modes, indexed, and integrated using the SAINT program [28]. Subsequently, the data were scaled and corrected for absorption using the SADABS program [29]. Detailed information can be found in Supplementary Materials (Table S1). The structures were determined by direct methods and refined using the full-matrix least squares technique on F^2 with anisotropic displacement parameters applied for non-hydrogen atoms. Hydrogen atoms in all compounds were positioned at calculated positions and refined within a riding model with fixed isotropic displacement parameters [$U_{iso}(H) = 1.5U_{eq}(C)$ for the CH_3-groups and $1.2U_{eq}(C)$ for the other groups]. All calculations were performed using the SHELXTL program [30] and OLEX2 program package [31].

In the structure of **2**, three CH_3CN molecules were identified to exhibit significant disorders and were subsequently excluded from the analysis using an OLEX2 solvent mask. Errors B in the structure of **2** are associated with the removal of these solvent molecules.

Crystallographic data for all compounds prepared have been deposited with the Cambridge Crystallographic Data Center, CCDC nos. 2286255–2286257 (for compounds **2**, **3**, **4**·2CH_3CN) and 2291145 (for L^2). Copies of this information may be obtained free of charge from the Director, CCDC, 12 Union Road, Cambridge CHB2 1EZ, UK (Fax: +44-1223-336033; e-mail: deposit@ccdc.cam.ac.uk or www.ccdc.cam.ac.uk, accessed on 2 August 2023).

2.9. Hirshfeld Surface Analysis

The Crystal Explorer 17.5 program [32] was employed to analyze the interactions occurring within the crystal. The donor–acceptor groups were visualized using a standard (high) surface resolution, and d_{norm} surfaces were mapped across a consistent color scale ranging from −0.640 (red) to 0.986 (blue) a.u.

3. Results and Discussion

In our previous study [23], we discovered that the *closo*-dodecaborate anion $[B_{12}H_{12}]^{2-}$, which has the lowest coordination ability among the polyhedral boron cluster anions $[B_nH_n]^{2-}$ (n = 6–12), may not effectively compete in zinc(II) and cadmium(II) complexation

when various organic and inorganic ligands are present in the solution—for instance, when nitrate ions or dimethylformamide molecules are present in excess. To address this challenge, we overcame the issue by utilizing previously synthesized complexes $[M(DMF)_6][B_{12}H_{12}]$ (where M = Zn(II), Cd(II)) as initial reagents [23,27]. Therefore, in this study, we conducted Zn(II) and Cd(II) complexation with benzimidazole derivatives L^1–L^3 in the presence of the $[B_{12}H_{12}]^{2-}$ anion, utilizing these compounds as our starting materials.

3.1. System $[M(DMF)_6][B_{12}H_{12}]$ (M = Zn(II), Cd(II))/L (L = L^1, L^2)

The reaction pathways for zinc(II) and cadmium(II) complexation with ligand L^1 containing the –CH=N– linker group and ligand L^2 with the $–CH_2–NH–$ linker group in the presence of the *closo*-dodecaborate anion are quite similar. In the case of cadmium(II) and ligand L^1, the mixed-ligand complex $[Cd(L^1)_2[B_{12}H_{12}]]$ was isolated with a boron cluster anion coordinated by the metal. However, for ligand L^2, we obtained a mixed-ligand cationic complex $[Cd(L^2)_2(CH_3CN)(H_2O)]^{2+}$ with the *closo*-dodecaborate anion serving as a counterion (Scheme 1). In contrast, for zinc(II), the initial components remained unreacted, regardless of U_{eq} the organic ligand used. It's worth noting that upon evaporating a solution containing $[Zn(DMF)_6][B_{12}H_{12}]$ and ligand L^2, single crystals of ligand L^2 suitable for X-ray diffraction studies precipitated (Figure S14).

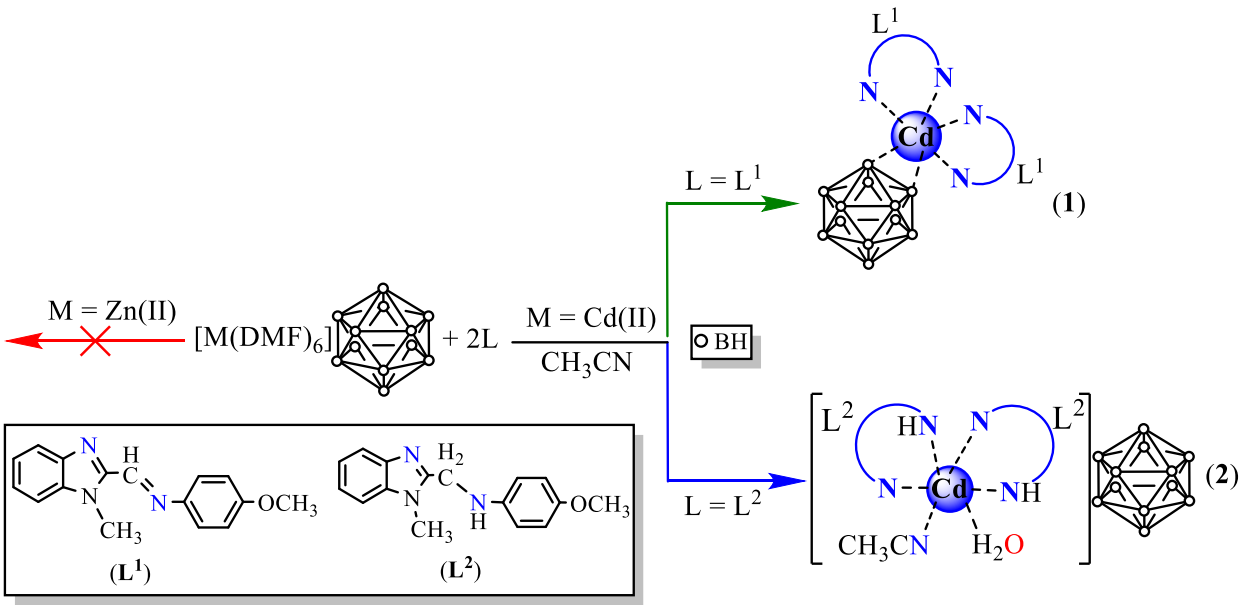

Scheme 1. Zinc(II) and cadmium(II) reactions with ligands L^1 and L^2 in the presence of the *closo*-dodecaborate anion $[B_{12}H_{12}]^{2-}$.

Note that a similar reaction of the cadmium(II) complexation with 1-(1-methylbenzimidazol-2-yl)-*N*-phenylmethanimine (L′) containing the –CH=N– linker group and the $[B_{12}H_{12}]^{2-}$ anion was described [27]. The authors isolated the mixed-ligand complex $[Cd(L')_2[B_{12}H_{12}]]$ with the coordinated *closo*-dodecaborate anion and determined its structure by X-ray diffraction.

The structure of complex **2** was determined using X-ray diffraction. The crystallographically independent part of the triclinic unit cell (space group *P*-1) of complex **2** contains the cationic complex $[CdL_2(CH_3CN)H_2O]^{2+}$ and two crystallographically independent halves of the $[B_{12}H_{12}]^{2-}$ anion (Figure 1). The cadmium(II) coordination environment is a strongly distorted octahedral and includes two nitrogen atoms of iminium (N_{im}), amino atoms (N_{amin}) of two azoligands, a nitrogen atom of acetonitrile (N_{CH3CN}), and one oxygen atom of a water molecule. The Cd–N_{im} bond lengths are 2.339(3) Å and 2.535(3) Å, and the Cd–N_{amin} bonds are 2.535(3) Å, 2.536(3) Å, Cd–N_{CH3CN} 2.536(3) Å, and Cd–O 2.339(3) Å.

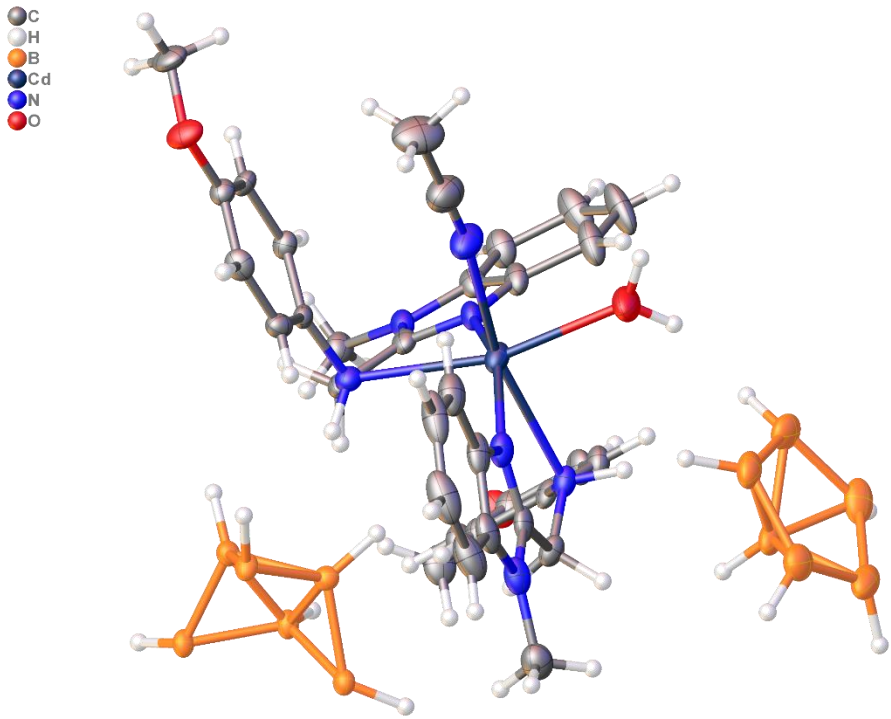

Figure 1. Crystallographically independent part of the unit cell of complex **2**.

Our analysis of the Hirshfeld surface of the *closo*-dodecaborate anions shows that cationic complexes are associated with the $[B_{12}H_{12}]^{2-}$ anions by weak OH. . .HB, NH. . .HB, CH. . .HB contacts (Figure 2a), forming 1D polymer chains in the crystal (Figure 2b). The H(O). . .H(B) and H(O). . .B distances are 2.2858(7) Å and 2.716(4) Å, respectively, whereas the H(N). . .H(B) and H(N). . .B contacts fall in the range 1.8537(4)–2.4691(6) Å and 2.446(3)–2.763(4) Å, respectively.

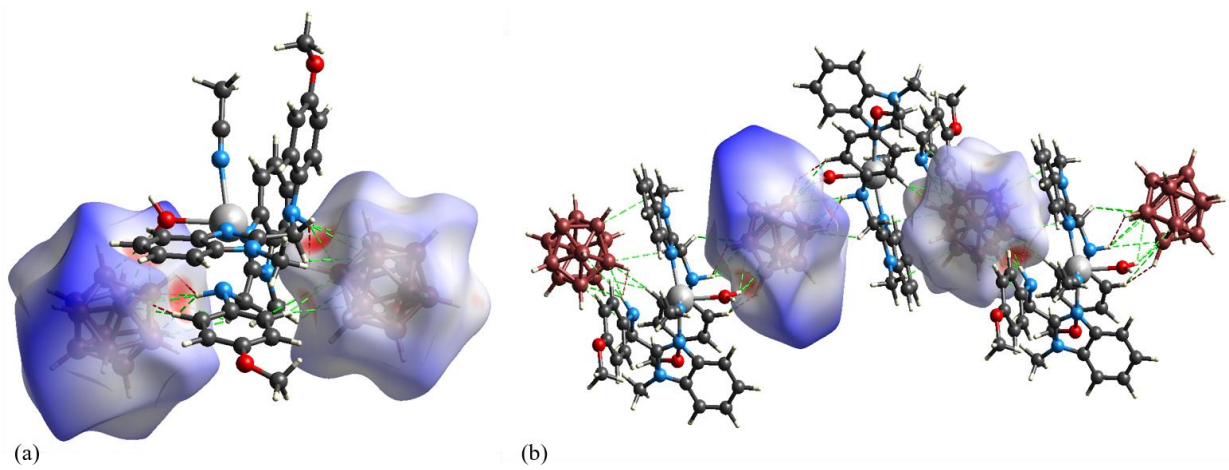

Figure 2. (**a**) OH. . .HB, NH. . .HB, and CH. . .HB contacts on the Hirshfeld surfaces of the $[B_{12}H_{12}]^{2-}$ anions, and (**b**) 1D polymer chains formed by these contacts. Dashed green lines and dashed red lines show H. . .B and H. . .H contacts shorter than the sum of the van der Waals radii of the corresponding atoms.

IR spectroscopy serves as an excellent tool for the qualitative identification of compound composition and preliminary structure determination. In particular, the presence of an absorption band of medium intensity $\nu(BH)_{MHB}$ at 2407 cm^{-1} in the IR spectrum of complex **1** indicates that the $[B_{12}H_{12}]^{2-}$ anion is coordinated by the metal. Additionally,

an intense absorption band assigned to the stretching vibrations of "free" BH bonds is observed in the region of 2510–2430 cm^{-1} (Figure S1).

In the IR spectra of ligand L^2 with the –CH_2–NH– linker group and complex **2**, there is a band of stretching vibrations of the NH bond, ν(NH) with two maxima observed at approximately 3260 and 3257 cm^{-1} (Figure S2). The coordinated state of the water molecule in complex **2** is evident through the presence of a broadened absorption band in the region of 3585–3510 cm^{-1}, which corresponds to the stretching vibrations of the OH groups of water molecules (Figure S2).

The coordinated state of organic ligands L^1 and L^2 is reflected in the IR spectra of the synthesized complexes by changes in the number and shift of absorption band maxima, as well as the redistribution of their intensities in the 1600–700 cm^{-1} region when compared to the IR spectra of uncoordinated ligands (Figures S1 and S2).

The coordinated state of ligands L^1 and L^2 can be inferred from the electronic absorption spectra of the isolated compound. Specifically, a bathochromic shift of the broadened intraligand charge transfer band in the UV-vis absorption spectra of complex **1** (~350 nm in the ligand vs. ~390 nm in the complex) (Figure S5) or a hypsochromic shift in the UV-vis absorption spectra of complex **2** (~310 nm in the ligand vs. ~290 nm in the complex) (Figure S6) reflects the effect of the central metal atom on the π-electron system of coordinated ligand molecules, and indicates the preservation of the ligand electronic structure.

3.2. System $[M(DMF)_6][B_{12}H_{12}]$ (M = Zn(II), Cd(II))/L^3

The zinc(II) and cadmium(II) complexation with ligand L^3, which contains the –N=CH– linker group, follows a fundamentally different pathway in the presence of the *closo*-dodecaborate anion $[B_{12}H_{12}]^{2-}$ compared to the processes described above. The study revealed the degradation of ligand L^3, which was visually evident. The initially bright yellow solution gradually changed to a pale yellow color after 4 h, eventually becoming almost completely colorless after 24 h. Consequently, for zinc(II), complex $[Zn(Bz\text{-}NH_2)_2(CH_3COO)_2]$ (**3**) was isolated. Notably, Bz-NH_2 (1-propyl-2-aminobenzimidazole) represents a fragment of the degraded ligand, and this complex does not contain the boron cluster anion. In the case of cadmium(II), a precipitate was obtained, consisting of a metal-free salt $(HBz\text{-}NH_2)_2[B_{12}H_{12}]\cdot 2CH_3CN$ (**4**·$2CH_3CN$), along with a cadmium(II) complex involving salicylaldehyde (Scheme 2).

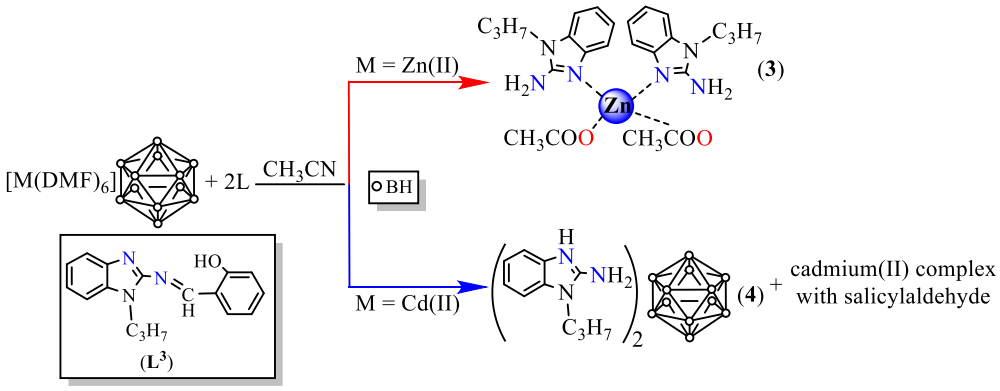

Scheme 2. Zinc(II) and cadmium(II) reaction with ligand L^3 in the presence of the *closo*-dodecaborate anion $[B_{12}H_{12}]^{2-}$.

It appears that the formation of compound **3** is influenced by the specific characteristics of the complexing metal, as well as the presence of both organic and inorganic bases. In this context, it's important to note that zinc(II) is considered a "harder" acid according to the Pearson's concept compared to cadmium(II), and it exhibits a high affinity for oxygen-containing species. As a result, the preferential formation of a bond with the oxygen-containing "hard" component of the system becomes more favorable compared to

forming a bond with the $[B_{12}H_{12}]^{2-}$ anion, which acts as a "soft" inorganic base. An analysis of the results presented above supports this hypothesis. When conducting complexation with stable "soft" organic ligands L^1 and L^2, which maintain their structures without degradation, the reaction with zinc(II) does not occur because of the absence of oxygen-containing degradation fragments.

According to the X-ray diffraction data, complex **3** crystallizes in the monoclinic system ($P2_1/n$). The coordination environment of the zinc(II) atom is distorted and tetrahedral; it includes two iminium nitrogen atoms from two ligands Bz-NH_2, and two oxygen atoms from two acetates (Figure 3). The Zn–N_{im} distances are 2.0059(14) Å and 2.0139(13) Å, and the Zn–O distances are 1.9444(12) Å and 1.9620(12) Å

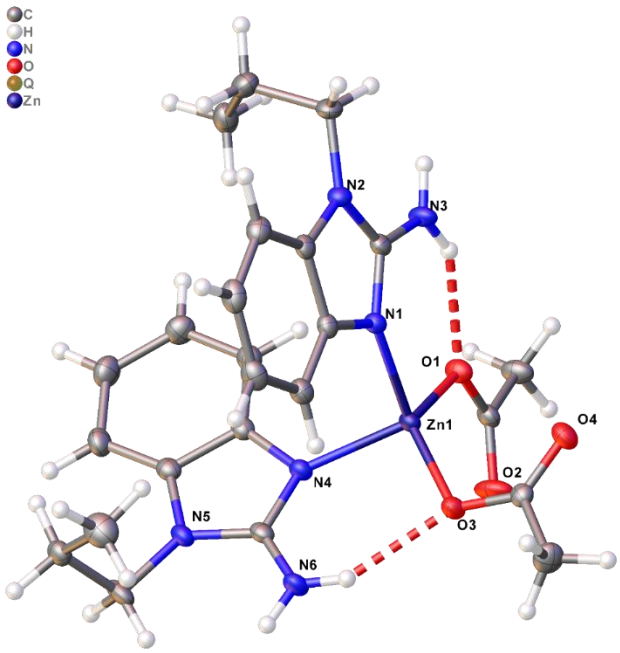

Figure 3. Structure of complex **3**.

Both ligands Bz-NH_2 participate in intra- and intermolecular NH. . .O hydrogen bonds with acetate ions in complex **3** (Table 1), forming 2D polymer planes (Figure 4). These planes are connected to each other due to π-π stacking interactions (centroid-centroid distance 3.718 Å, shift distance 1.548 Å, angle 0.00°).

Table 1. Hydrogen bonds in the structure of complex **3**.

D–H–A	d(H–A)/Å	d(D–A)/Å	D–H–A/°
N3–H3A–O1	2.11	2.8771(19)	145.8
N6–H6A–O3	2.11	2.8976(18)	148.4
N6–H6B–O2 [1]	1.95	2.8131(18)	166.6

[1] $1-x, 1-y, 1-z$.

The data of the IR spectrum of complex **3** align with the findings obtained by X-ray diffraction. Firstly, the appearance of absorption bands $\nu_{as}(NH)_{NH2}$ at 3333 cm^{-1} and $\nu_s(NH)_{NH2}$ at 3189 cm^{-1}, compared to the IR spectrum of ligand L^3, indicates the formation of a compound containing an NH_2 group, specifically 1-propyl-2-aminobenzimidazole (Figure S3). Secondly, the presence of a strong absorption band of stretching vibrations $\nu(CO)_{COO}$ at 1663 cm^{-1} in a lower frequency region compared to the position of this absorption band in uncoordinated acetate ($\nu(COO)_{COOH}$~1700 cm^{-1}) suggests the coordination of the acetate group in complex **3**.

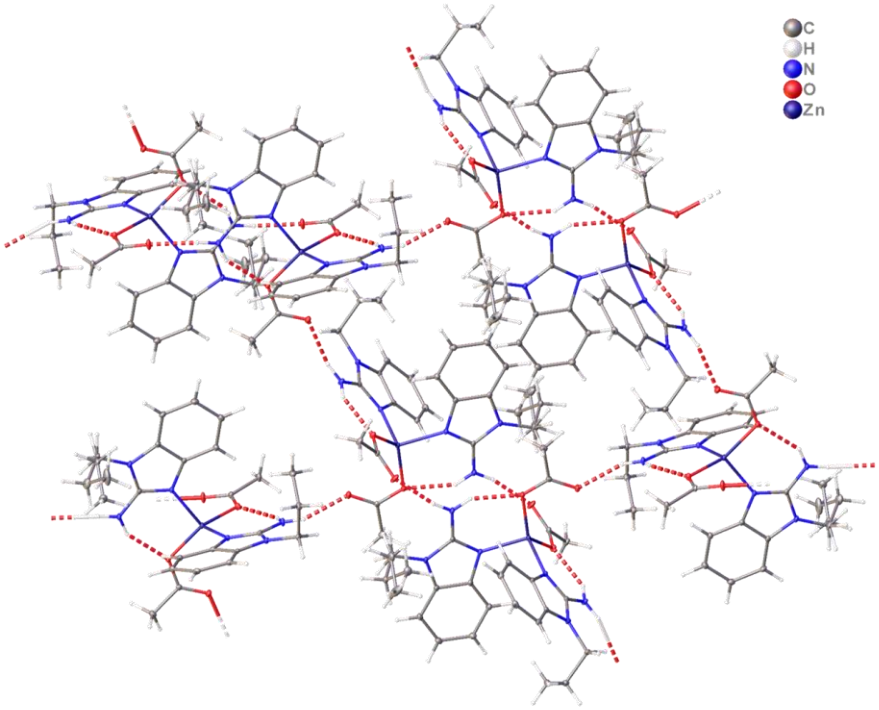

Figure 4. 2D polymer planes in crystal **3** formed by NH. . .O hydrogen bonds.

The composition of the products resulting from the reaction of cadmium(II) with ligand L^3 in the presence of the *closo*-dodecaborate anion was identified based on IR spectroscopy and X-ray diffraction data.

According to the X-ray diffraction data, one of the products is a salt-containing protonated 1-propyl-2-aminobenzimidazole (HBz-NH_2) as a cation, whereas the *closo*-dodecaborate anion acts as a counterion. It's worth noting that the protonation of nitrogen-containing ligands during complexation in the presence of *closo*-borohydride anions is not without precedent. In [33,34], the authors describe the isolation of salts $(H_2phen)[B_{10}H_{10}]$ and $(Hbpa)_2[B_{12}H_{11}OH]$ during the cobalt(II) complexation in the $CoCl_2$/phen/$[B_{10}H_{10}]^{2-}$ system and lead(II) complexation in the $Cs_2[B_{12}H_{11}OH]/Pb(NO_3)_2$/bpa system, respectively.

The crystallographically independent part of the triclinic unit cell (*P*-1) of salt **4**·$2CH_3CN$ contains one HBz-NH_2 cation, half of the $[B_{12}H_{12}]^{2-}$ anion, and an acetonitrile molecule (Figure 5a). One of the hydrogen atoms of the amino group of the cation and the iminium proton form short NH...HB contacts with the anion, linking cations and anions into a 1D polymer chain along axis *c* (Figure 5b). The second hydrogen atom of the amino group of the cation is hydrogen bonded to the solvate molecule of acetonitrile. The cations are connected by π-π stacking interactions (centroid-centroid distance 3.761 Å, shift distance 1.576 Å, angle 0.00°). In addition, the chains are connected by the CH...HB contacts between cations and anions (white spots on the Hirshfeld surface of the anion).

However, in the IR spectrum of the resulting precipitate, in addition to the absorption bands characteristic of a compound containing NH and NH_2 groups (broadened absorption band with maxima at 3340, 3334, 3298, 3225 cm^{-1}) and the $[B_{12}H_{12}]^{2-}$ anion (intense absorption band with a maximum at 2470 cm^{-1}), there is a band of stretching vibrations of the free OH group ν(OH) at 3605, 3566 cm^{-1}, as well as an intense absorption band at 1663 cm^{-1}, related to stretching vibrations ν(C=O) of the coordinated aldehyde group (Figure S4). Considering that during complexation, the ligand L^3 is degraded and one of the products is 1-propyl-2-aminobenzimidazole, the second product is probably salicylaldehyde. Therefore, based on the IR spectroscopy data, the second product is likely to be a cadmium(II) complex with salicylaldehyde.

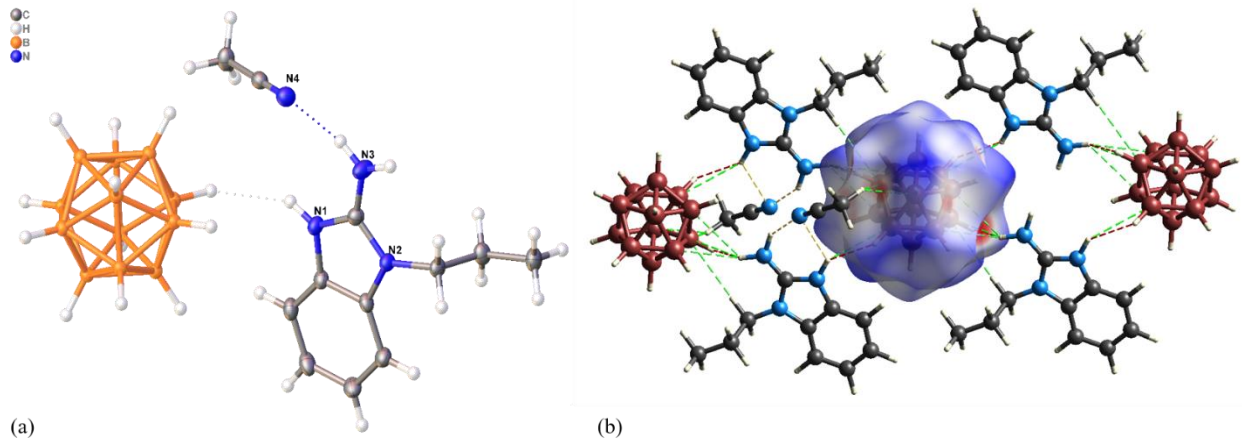

Figure 5. (**a**) Structures of the cation and anion in salt **4**·2CH_3CN, (**b**) Hirshfeld surface of the $[B_{12}H_{12}]^{2-}$ anion. The dotted green, red, and yellow lines show H. . .B, H. . .H, and H. . .N contacts shorter than the sum of the Van der Waals radii of the corresponding atoms.

Note that several complexes of transition metals, such as Cd(II), Ni(II), Co(II), Mg(II) [35], Fe(III) [36], Re(I) [37], and *N*-(benzimidazol-2-yl)salicylaldimine containing the linker –N=CH– group—like ligand L^3 used in this work—are known. In the case of metals M(II), this ligand was formed during complexation in the M^+/salicylaldehyde/2-aminobenzimidazole system, while for iron(III) and rhenium(I), this ligand was used as an individual compound. Moreover, this ligand retains its structure in the Fe(III) and Re(I) complexes. According to the methodology presented by the authors [36], we tried to realize the above-described cadmium(II) complexation in methanol. However, the initially bright yellow solution also became almost colorless after 24 h. Evaporation of the reaction solution for 48 h led to the formation of a precipitate, the IR spectrum of which completely coincided with that shown in Figure S4.

For compound **3**, the UV spectrum of a suspension in glycerol was recorded and analyzed. The disappearance of the absorption band related to intraligand charge transfer in the electronic absorption spectrum of **3** indicates the disappearance of the π-conjugated double bond system as a result of ligand degradation.

4. Conclusions

In this study, we investigated the process of zinc(II) and cadmium(II) complexation with a set of benzimidazole derivatives featuring different linker groups: *N*-(4-methoxyphenyl)-1-(1-methylbenzimidazol-2-yl)methanimine (L^1) (the –CH=N– linker group), 4-methoxy-*N*-[(1-methylbenzimidazol-2-yl)methyl]aniline (L^2) (the –CH_2–NH– linker group), and 2-[(*E*)-(1-propylbenzimidazol-2-yl)iminomethyl]phenol (L^3) (the –N=CH– linker group), all in the presence of the *closo*-dodecaborate anion. We observed that both the choice of the complexing metal and the nature of the linker group have significant effects on the course of complexation.

(i) The reaction between zinc(II), the "soft" inorganic anion $[B_{12}H_{12}]^{2-}$, and "soft" organic ligands L^1 and L^2, which retain their structures during the complexation, did not occur. Mixed-ligand complexes were exclusively formed with cadmium(II). Specifically, complexes $[Cd(L^1)_2[B_{12}H_{12}]]$ with the coordinated $[B_{12}H_{12}]^{2-}$ anion and $[Cd(L^2)_2(CH_3CN)(H_2O)][B_{12}H_{12}]$ with the boron cluster anion as a counterion were isolated. The latter complex was characterized by X-ray diffraction.

(ii) Ligand L^3 was found to undergo degradation, yielding 1-propyl-2-aminobenzimidazole (Bz-NH_2) and salicylaldehyde. Consequently, we isolated zinc(II) complex $[Zn(Bz\text{-}NH_2)_2(CH_3COO)_2]$ and salt $(HBz\text{-}NH_2)_2[B_{12}H_{12}]\cdot 2CH_3CN$, and their structures were determined using X-ray diffraction.

Analysis of the electronic absorption spectra of the obtained compounds showed that the structures of ligands L^1 and L^2 are preserved in their complexes. In the case of ligand L^3,

cleavage of the linker bond –N=CH– during the complexation leads to the disappearance of π-conjugation of the electronic structure of the ligand.

Supplementary Materials: The following supporting information can be downloaded at: https://www.mdpi.com/article/10.3390/cryst13101449/s1, Table S1: Crystal data and structure refinement for **2, 3,** and **4**·2CH_3CN; Figure S1: IR spectra of ligand L^1 (blue) and complex **1** (red); Figure S2: IR spectra of ligand L^2 (blue) and complex **2** (red); Figure S3: IR spectra of ligand L^3 (blue) and complex **3** (red); Figure S4: IR spectra of ligand L^3 (blue) and a precipitate containing $(HBz\text{-}NH_2)_2[B_{12}H_{12}]$ (**4**) and a cadmium(II) complex with salicylaldehyde (red); Figure S5: UV-vis absorption spectra of ligand L^1 (blue) and complex **1** (red); Figure S6: UV-vis absorption spectra of ligand L^2 (blue) and complex **2** (red); Figure S7: UV-vis absorption spectra of ligand L^3 (blue) and complex **3** (red); Figure S8: ^{1}H NMR spectrum of *N*-(4-methoxyphenyl)-1-(1-methylbenzimidazol-2-yl)methanimine (L^1); Figure S9: ^{1}H NMR spectrum of 4-methoxy-*N*-[(1-methylbenzimidazol-2-yl)methyl]aniline (L^2); Figure S10: ^{1}H NMR spectrum of 2-[(*E*)-(1-propylbenzimidazol-2-yl)iminomethyl]phenol (L^3); Figure S11: ^{13}C NMR spectrum of *N*-(4-methoxyphenyl)-1-(1-methylbenzimidazol-2-yl)methanimine (L^1); Figure S12: ^{13}C NMR spectrum of 4-methoxy-*N*-[(1-methylbenzimidazol-2-yl)methyl]aniline (L^2); Figure S13: ^{13}C NMR spectrum of 2-[(*E*)-(1-propylbenzimidazol-2-yl)iminomethyl]phenol (L^3); Figure S14: Structure of ligand L^2.

Author Contributions: Conceptualization, A.S.B. and N.T.K.; methodology, E.A.M. and L.N.D.; formal analysis, A.S.K., L.V.G. and Y.V.K.; investigation, S.E.N., N.A.K. and Y.V.K.; data curation, E.A.M., V.V.A. and L.N.D.; writing—original draft preparation, S.E.N. and N.A.K.; writing—review and editing, V.V.A. and A.S.B.; visualization, A.S.K. and L.V.G.; supervision, N.T.K. All authors have read and agreed to the published version of the manuscript.

Funding: This research received no external funding.

Data Availability Statement: The spectral data in this study are available in the Supplementary Materials. The deposition numbers for compounds **2**–**4**·2CH_3CN are CCDC 2286255–2286257, for ligand L^2 is 2291145. The data can be obtained free of charge via www.ccdc.cam.ac.uk/data_request/cif (accessed on 2 August 2023), by emailing deposit@ccdc.cam.ac.uk, or by contacting The Cambridge Crystallographic Data Centre, 12 Union Road, Cambridge CB2 1EZ, UK; fax: +44-1223-336033.

Acknowledgments: This work was supported by the Ministry of Science and Higher Education of the Russian Federation as part of the State Assignment of the Kurnakov Institute of General and Inorganic Chemistry, Russian Academy of Sciences, in the field of fundamental research. The X-ray diffraction studies were performed at the Shared Facility Center of the Kurnakov Institute (IGIC RAS) within the framework of the State Assignment of the Kurnakov Institute in the field of fundamental scientific research. Synthesis of benzimidazole derivatives and NMR studies were performed in the Institute of Physical and Organic Chemistry, Southern Federal University and supported by the Ministry of Science and Education of the Russian Federation (grant FENW-2023-0011).

Conflicts of Interest: The authors declare no conflict of interest.

References

1. Chkirate, K.; Essassi, E.M. Pyrazole and Benzimidazole Derivatives: Chelating Properties Towards Metals Ions and their Applications. *Curr. Org. Chem.* **2022**, *26*, 1735–1766. [CrossRef]
2. Al Awadh, A.A. Biomedical applications of selective metal complexes of indole, benzimidazole, benzothiazole and benzoxazole: A review (From 2015 to 2022). *Saudi Pharm. J.* **2023**, *31*, 101698. [CrossRef] [PubMed]
3. Ugwu, D.I.; Conradie, J. Anticancer properties of complexes derived from bidentate ligands. *J. Inorg. Biochem.* **2023**, *246*, 112268. [CrossRef] [PubMed]
4. Suárez-Moreno, G.V.; Hernández-Romero, D.; García-Barradas, Ó.; Vázquez-Vera, Ó.; Rosete-Luna, S.; Cruz-Cruz, C.A.; López-Monteon, A.; Carrillo-Ahumada, J.; David Morales-Morales, D.; Colorado-Peralta, R. Second and third-row transition metal compounds containing benzimidazole ligands: An overview of their anticancer and antitumour activity. *Coord. Chem. Rev.* **2022**, *472*, 214790. [CrossRef]
5. Mahmood, K.; Hashmi, W.; Ismail, H.; Mirza, B.; Twamley, B.; Akhter, Z.; Rozas, I.; Baker, R.J. Synthesis, DNA binding and antibacterial activity of metal(II) complexes of a benzimidazole Schiff base. *Polyhedron* **2019**, *157*, 326–334. [CrossRef]
6. Šindelář, Z.; Kopel, P. Bis(benzimidazole) Complexes, Synthesis and Their Biological Properties: A Perspective. *Inorganics* **2023**, *11*, 113. [CrossRef]

7. Darwish, N.B.; Kurdi, A.; Alshihri, S.; Tabbakh, T. Organic heterocyclic-based colorimetric and fluorimetric chemosensors for the detection of different analytes: A review (from 2015 to 2022). *Mater. Today Chem.* **2023**, *27*, 101347. [CrossRef]
8. Jindal, G.; Vashisht, P.; Kaur, N. Benzimidazole appended optical sensors for ionic species: Compilation of literature reports from 2017 to 2022. *Results Chem.* **2022**, *4*, 100551. [CrossRef]
9. Cruz-Navarro, A.; Hernández-Romero, D.; Flores-Parra, A.; Rivera, J.M.; Castillo-Blum, S.E.; Colorado-Peralta, R. Structural diversity and luminescent properties of coordination complexes obtained from trivalent lanthanide ions with the ligands: Tris ((1H-benzo[d]imidazol-2-yl)methyl)amine and 2,6-bis(1H-benzo[d]imidazol-2-yl)pyridine. *Coord. Chem. Rev.* **2021**, *427*, 213587. [CrossRef]
10. Nair, P.; Jayaraj, A.; Swamy, C.A. Recent Advances in Benzimidazole Based NHC-Metal Complex Catalysed Cross-Coupling Reactions. *ChemistrySelect* **2022**, *7*, e202103517. [CrossRef]
11. Coghi, P.; Hosmane, N.S.; Zhu, Y. Next generation of boron neutron capture therapy (BNCT) agents for cancer treatment. *Med. Res. Rev.* **2023**, *43*, 1809–1830. [CrossRef] [PubMed]
12. Hou, W.; Yang, M.; Guo, Y.; Ma, Y.; Guo, M.; Xiao, Y.; Han, G. Synergistic effects of caesium *closo*-dodecaborate on buried interface for efficient and stable perovskite solar cells. *J. Colloid Interface Sci.* **2023**, *645*, 472–482. [CrossRef] [PubMed]
13. Chen, C.; Chen, Z.; Zhang, M.; Zheng, S.; Zhang, W.; Li, S.; Pan, F. *Closo*-$[B_{12}H_{12}]^{2-}$ Derivatives with Polar Groups As Promising Building Blocks in Metal-Organic Frameworks for Gas Separation. *ChemSusChem.* **2023**, *16*, e202300434. [CrossRef]
14. Corona-López, M.M.; Muñoz-Flores, B.M.; Chaari, M.; Nuñez, R.; Jiménez-Pérez, V.M. Far-Red and Near-Infrared Boron Schiff Bases (BOSCHIBAs) Dyes Bearing Anionic Boron Clusters. *Eur. J. Inorg. Chem* **2021**, *2021*, 2047–2054. [CrossRef]
15. Sun, W.; Jin, Y.; Wu, Y.; Lou, W.; Yuan, Y.; Duttwyler, S.; Wang, L.; Zhang, Y. A new boron cluster anion pillared metal organic framework with ligand inclusion and its selective acetylene capture properties. *Inorg. Chem. Front.* **2022**, *9*, 5140–5147. [CrossRef]
16. Hattori, Y.; Ishimura, M.; Ohta, Y.; Takenaka, H.; Kawabata, S.; Kirihata, M. Dodecaborate Conjugates Targeting Tumor Cell Overexpressing Translocator Protein for Boron Neutron Capture Therapy. *ACS Med. Chem. Lett.* **2022**, *13*, 50–54. [CrossRef]
17. Hagemann, H. Boron Hydrogen Compounds: Hydrogen Storage and Battery Applications. *Molecules* **2021**, *26*, 7425. [CrossRef]
18. Zhang, Z.; Zhao, Z.; Wang, B.; Zhang, J. Boron based hypergolic ionic liquids: A review. *Green Energy Environ.* **2021**, *6*, 794–822. [CrossRef]
19. Zhao, X.; Yang, Z.; Chen, H.; Wang, Z.; Zhou, X.; Zhang, H. Progress in three-dimensional aromatic-like *closo*-dodecaborate. *Coord. Chem. Rev.* **2021**, *444*, 214042. [CrossRef]
20. Tiritiris, I.; Schleid, T. Zu den Kristallstrukturen der Übergangsmetall(II)-Dodekahydro-*closo*-Dodekaborat-Hydrate $Cu(H_2O)_{5,5}[B_{12}H_{12}]\cdot 2{,}5\ H_2O$ und $Zn(H_2O)_6[B_{12}H_{12}]\cdot 6\ H_2O$. *Z. Anorg. Allg. Chem.* **2008**, *634*, 317–324. [CrossRef]
21. Tiritiris, I.; Schield, T. Synthese und Kristallstruktur von Cadmium-Dodekahydro-*closo*-Dodekaborat-Hexahydrat, $Cd(H_2O)_6[B_{12}H_{12}]$. *Z. Anorg. Allg. Chem.* **2005**, *631*, 1593–1596. [CrossRef]
22. Lacroix, M.R.; Bukovsky, E.V.; Lozinsek, M.; Folsom, T.C.; Newell, B.S.; Liu, Y.; Peryshkov, D.V.; Strauss, S.H. Manifestations of Weak O−H···F Hydrogen Bonding in $M(H_2O)_n(B_{12}F_{12})$ Salt Hydrates: Unusually Sharp Fourier Transform Infrared ν(OH) Bands and Latent Porosity (M = Mg−Ba, Co, Ni, Zn). *Inorg. Chem.* **2018**, *57*, 14983–15000. [CrossRef] [PubMed]
23. Korolenko, S.E.; Kubasov, A.S.; Goeva, L.V.; Avdeeva, V.V.; Malinina, E.A.; Kuznetsov, N.T. Reactivity of the dodecahydro-*closo*-dodecaborate anion in zinc(II) and cadmium(II) complexation at the presence of azaheterocyclic ligands. *Inorg. Chim. Acta* **2021**, *527*, 120587. [CrossRef]
24. Groutchik, K.; Jaiswal, K.; Dobrovetsky, R. An air-stable, Zn^{2+}-based catalyst for hydrosilylation of alkenes and alkynes. *Org. Biomol. Chem.* **2021**, *19*, 5544–5550. [CrossRef]
25. Zhang, Z.; Zhang, Y.; Li, Z.; Jiao, N.; Liu, L.; Zhang, S. $B_{12}H_{12}{}^{2-}$-Based Metal (Cu^{2+}, Ni^{2+}, Zn^{2+}) Complexes as Hypergolic Fuels with Superior Hypergolicity. *Eur. J. Inorg. Chem.* **2018**, *2018*, 981–986. [CrossRef]
26. Wehmschulte, R.J.; Bayliss, B.; Reed, S.; Wesenberg, C.; Morgante, P.; Peverati, R.; Neal, S.; Chouinard, C.D.; Tolosa, D.; Powell, D.R. Zinc Ammonio-dodecaborates: Synthesis, Lewis Acid Strength, and Reactivity. *Inorg. Chem.* **2022**, *61*, 7032–7042. [CrossRef]
27. Korolenko, S.E.; Kubasov, A.S.; Khan, N.A.; Goeva, L.V.; Burlov, A.S.; Divaeva, L.N.; Malinina, E.A.; Avdeeva, V.V.; Zhizhin, K.Y.; Kuznetsov, N.T. Boron Cluster Anion $[B_{12}H_{12}]^{2-}$ in Zinc(II) and Cadmium(II) Complexation at the Presence of N-Donor Heterocyclic Ligands. *J. Clust. Sci.* **2023**, *34*, 933–942. [CrossRef]
28. Bruker. *SAINT*; Bruker AXS Inc.: Madison, WI, USA, 2018.
29. Krause, L.; Herbst-Irmer, R.; Sheldrick, G.M.; Stalke, D. Comparison of Silver and Molybdenum Microfocus X-Ray Sources for Single-Crystal Structure Determination. *J. Appl. Crystallogr.* **2015**, *48*, 3–10. [CrossRef]
30. Sheldrick, G.M. Crystal Structure Refinement with SHELXL. *Acta Crystallogr. Sect. C Struct. Chem.* **2015**, *71*, 3–8. [CrossRef]
31. Dolomanov, O.V.; Bourhis, L.J.; Gildea, R.J.; Howard, J.A.K.; Puschmann, H. OLEX2: A complete structure solution, refinement and analysis program. *J. Appl. Crystallogr.* **2009**, *42*, 339–341. [CrossRef]
32. Turner, M.J.; McKinnon, J.J.; Wolff, S.K.; Grimwood, D.J.; Spackman, P.R.; Jayatilaka, D.; Spackman, M.A. *CrystalExplorer 17.5*; University of Western Australia: Perth, Australia, 2017.
33. Avdeeva, V.V.; Vologzhanina, A.V.; Malinina, E.A.; Kuznetsov, N.T. Dihydrogen Bonds in Salts of Boron Cluster Anions $[B_nH_n]^{2-}$ with Protonated Heterocyclic Organic Bases. *Crystals* **2019**, *9*, 330. [CrossRef]
34. Malinina, E.A.; Kubasov, A.S.; Matveev, E.Y.; Nichugovskii, A.I.; Nikiforova, S.E.; Goeva, L.V.; Avdeeva, V.V.; Zhizhin, K.Y.; Kuznetsov, N.T. Hydroxy-substituted *closo*-dodecaborate anion $[B_{12}H_{11}OH]^{2-}$ in silver(I) and lead(II) complexation in the presence of azaheterocyclic ligands L. *Polyhedron* **2023**, *242*, 116516. [CrossRef]

35. Cao, W.; Zheng, X.-J.; Sun, J.-P.; Wong, W.-T.; Fang, D.-C.; Zhang, J.-X.; Jin, L.-P. A Highly Selective Chemosensor for Al(III) and Zn(II) and Its Coordination with Metal Ions. *Inorg. Chem.* **2014**, *53*, 3012–3021. [CrossRef] [PubMed]
36. Murali, M.; Nayak, S.; Costa, J.S.; Ribas, J.; Mutikainen, I.; Turpeinen, U.; Clémancey, M.; Garcia-Serres, R.; Latour, J.-M.; Gamez, P.; et al. Discrete Tetrairon(III) Cluster Exhibiting a Square-Planar $Fe_4(\mu_4\text{-O})$ Core: Structural and Magnetic Properties. *Inorg. Chem.* **2010**, *49*, 2427–2434. [CrossRef]
37. Booysen, I.N.; Ismail, M.B.; Munro, O.Q. Mono- and dinuclear rhenium(I) compounds with bidentate benzimidazole chelators. *Inorg. Chem. Commun.* **2013**, *30*, 168–172. [CrossRef]